THE POLE PROFILE DESIGN OF THE ACOL QUADRUPOLES

M. R. Harold and H. H. Umstatter

20/2/85

Introduction

ACOL is a large - acceptance 3.5GeV/c antiproton collector, taking the form of storage ring, and being situated around the antiproton accumulator (AA). The magnetic guide field is provided by dipoles and quadrupoles, two of the latter being "special" and not included in this report. The remaining 54 quadrupoles have been designed in collaboration with Rutherford Appleton Laboratory using the computer programmes MAGNET, PE2D and TOSCA. The quadrupoles divide into two broad types: the narrow (QN), containing a pure quadrupole field, and the wide (QW) which contains two different sextupole components. In all, there are seven different families, each family characterised by its own combination of field gradient and sextupole term. All the quadrupoles are to be electrically in series, there being three subsidiary trim power supplies.

The Narrow Quadrupole

As its name implies, this magnet had to be kept reasonably narrow in order to avoid clashing with either the existing AA ring or the building wall. A solution was found in two dimensions using MAGNET: this had the virtue of 45° symmetry, but on the other hand the fields at the root of the pole were rather high.

The QN parameters as originally specified are given in Table 1 below. There are three families, in two of which the quadrupoles are displaced radially in order to provide bending as well as focussing. The nominal inscribed radius is 110 mm. (This is the radius of an equivalent hyperbolic pole. The actual radius is larger due to a 12-pole end field correction).

TABLE 1

QN Parameters

Name	Number off	Gradient (T/m)	Mag. Length (m)	Bend Angle (m rad)	Turns/Pole	Good field region (mm)	
						H	V
QN1-3	12	6.917	0.7	0	19	52	52
QN4	7	6.559	0.7	30	17	52 + 76	38
QN5	7	6.144	0.7	18	15	35 + 49	49

Using PE2D and a hyperbolic pole profile, pole-edge shims were adjusted to obtain a field gradient uniform to 1 in 10^3 out to a radius of 130 mm. The quadrupole was then modelled on TOSCA (a three-dimensional electromagnetic programme) using a mesh which is illustrated in Fig 1. The B-H curve used was that of a good, low-carbon steel (the PE2D default curve), but allowance was made for the packing factor by multiplying the B-valves by 0.95. The field distribution given by TOSCA in the magnet centre was agreed very well with that given by PE2D (see Fig 2), but the reduced gradient value (for the same ampere-turns) showed that the return flux due to the end fringe field was having an appreciable effect.

The half-length of the QN was 300 mm. The fields were integrated out to 970 mm from the magnet centre, and the 12-pole content determined by analysis. The reverse of this component was then multiplied by the ratio L_{eff}/L_{iron} and incorporated into the pole profile. This was done on the assumption that alterations made to the iron dimensions were effective over the iron length only. The shims were then adjusted to obtain the required gradient-integral uniformity. The results at three different energizations, and for a fixed μ of 10,000 in the steel, are shown in Fig 3. In practice, the magnet cores will be 607 mm long, and when this is allowed for the magnetization curve as predicted by TOSCA is shown in Fig 4. The profile is defined in Fig 5.

The Wide Quadrupoles

The parameters of the wide quadrupoles are given below in Table II.

TOSCA NAME	Lattice Name	Number off	Gradient (T/m)	Length (m)	Turn/pole	K'/K	Good field region H	Good field region V
QWS	QFW8	8	6.47	0.75	26	0.617	162	33
QWSS	QDW7	8	5.85	"	22	1.464	90	54
"	QFW6	8	5.32	"	20	"	82	32
"	QDW9	4	4.61	"	17	"	95	51

For convenience we use here the TOSCA job names of QWS and QWSS to distinguish between quadrupoles with sextupole (S) and strong sextupole (SS) components. There are thus two distinct sets of profiles required, but the yokes and winding configuration are identical for the QWS and QWSS. The nominal bore radius is 132 mm.

Because of the large horizontal aperture required in QWS, an asymmetric design was adopted, and the same procedure as that used for the QN was followed. In mounting the problem on TOSCA, 180° of the magnet had to be defined because of the ultimate incorporation of the sextupole term (See Fig 6). For the QWSS, advantage was taken of the smaller horizontal aperture needed by reducing the pole width.

First, symmetry with respect to the vertical plane was assumed and the end effects (8 and 12 pole) were corrected as in the QN. Then the desired values of 6-pole were included in the two profiles. In the case of the QWS, the higher-field side required no further shimming; however, because of the reduced saturation effects on the other side, the field was too high and some metal had to be removed. This took the form of a 16-pole correction for $x < -140$ mm, being smoothly merged with the rest of the profile. Fig 7 shows PE2D and TOSCA (at $z = 0$) to agree fairly well, though not as well as in the case of the QN. Fig 8 gives the results for the gradient integrals; if one subtracts from the raw TOSCA data the differences between PE2D and TOSCA at $z = 0$, the continuous curve is obtained. The final QWS profiles are shown in Fig 9.

The same procedure was carried out for the QWSS. The mesh used (see Fig 10) was a slightly modified version of the QWS mesh. With the 6-, 8- and 12- pole terms in the pole profiles it was found that the resultant sextupole field component was dependent on the quadrupole energization. The 6-pole term was therefore adjusted slightly so as to be more nearly correct in the middle of the range of gradient values required. Fig 11 compares PE2D with TOSCA at $z = 0$, Fig 12 gives the integral results for different ampere-turns values, and Fig 13 shows the final profiles.

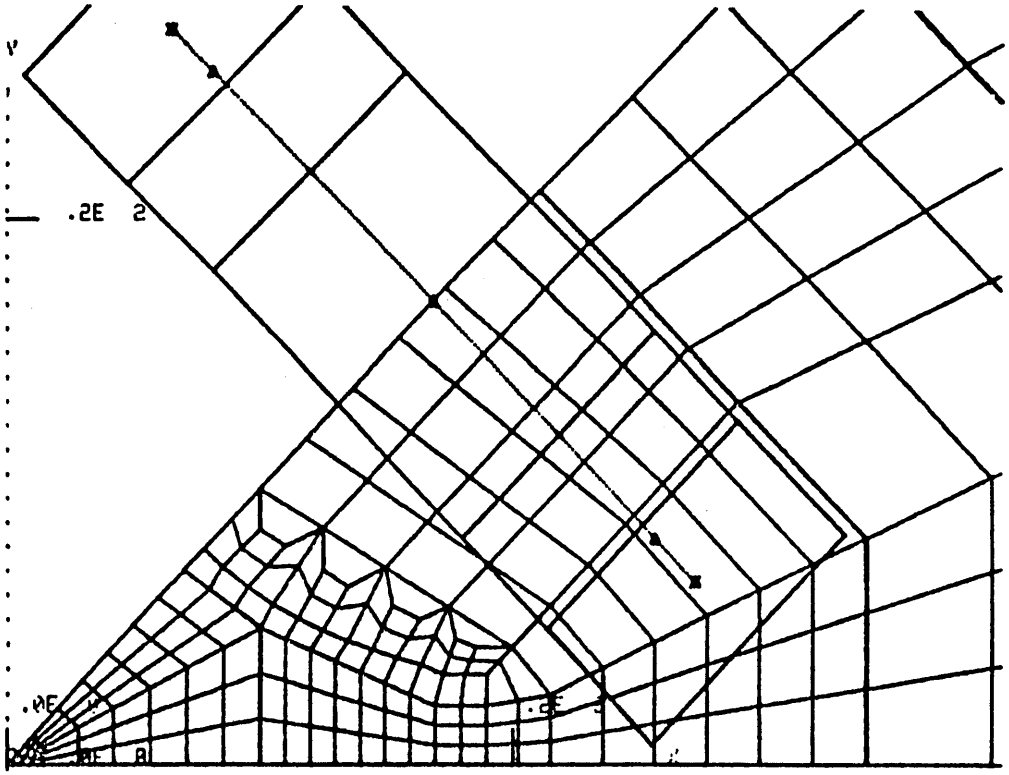

Fig 1. TOSCA mesh for QN

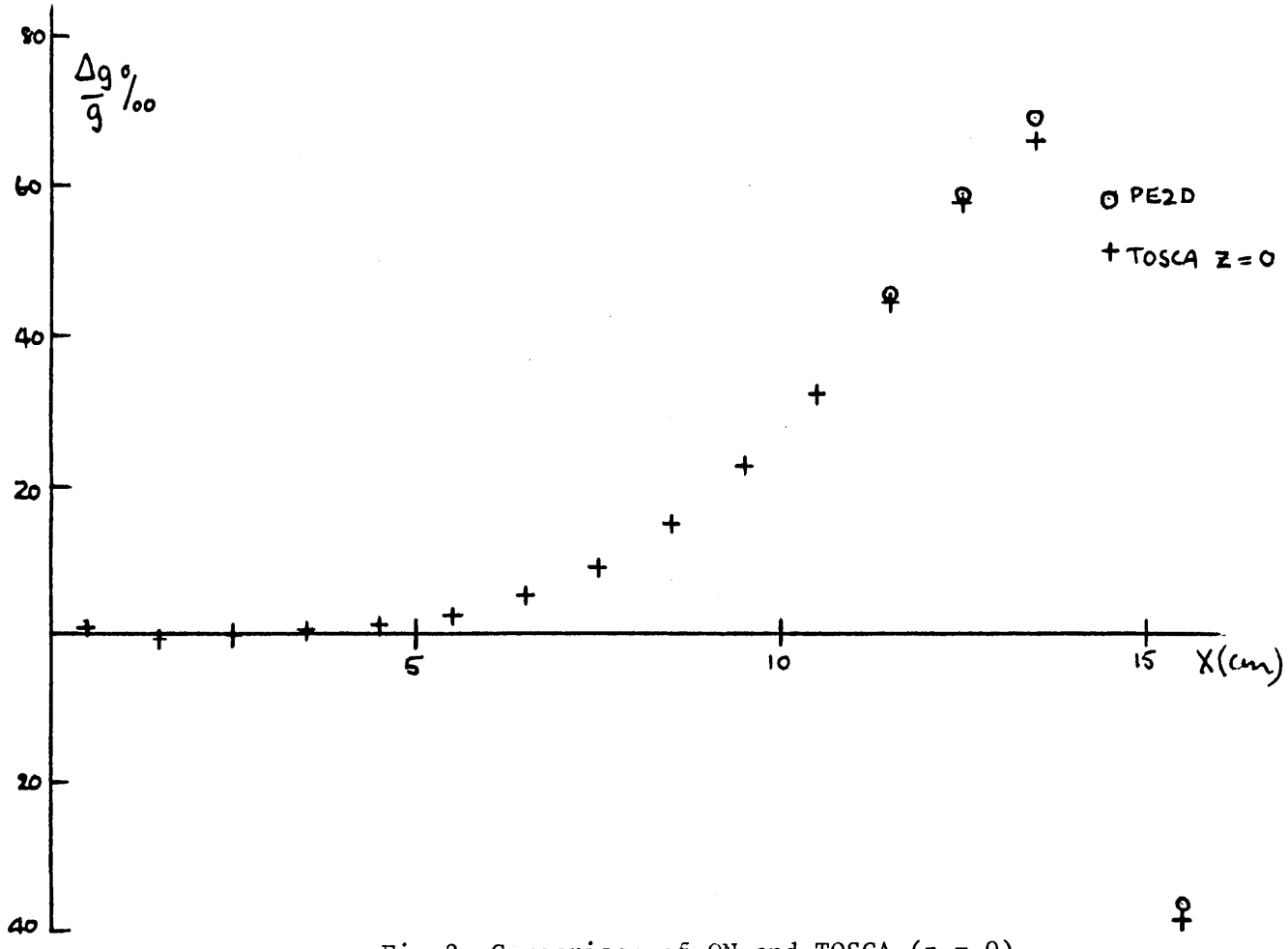

Fig 2. Comparison of QN and TOSCA (z = 0)

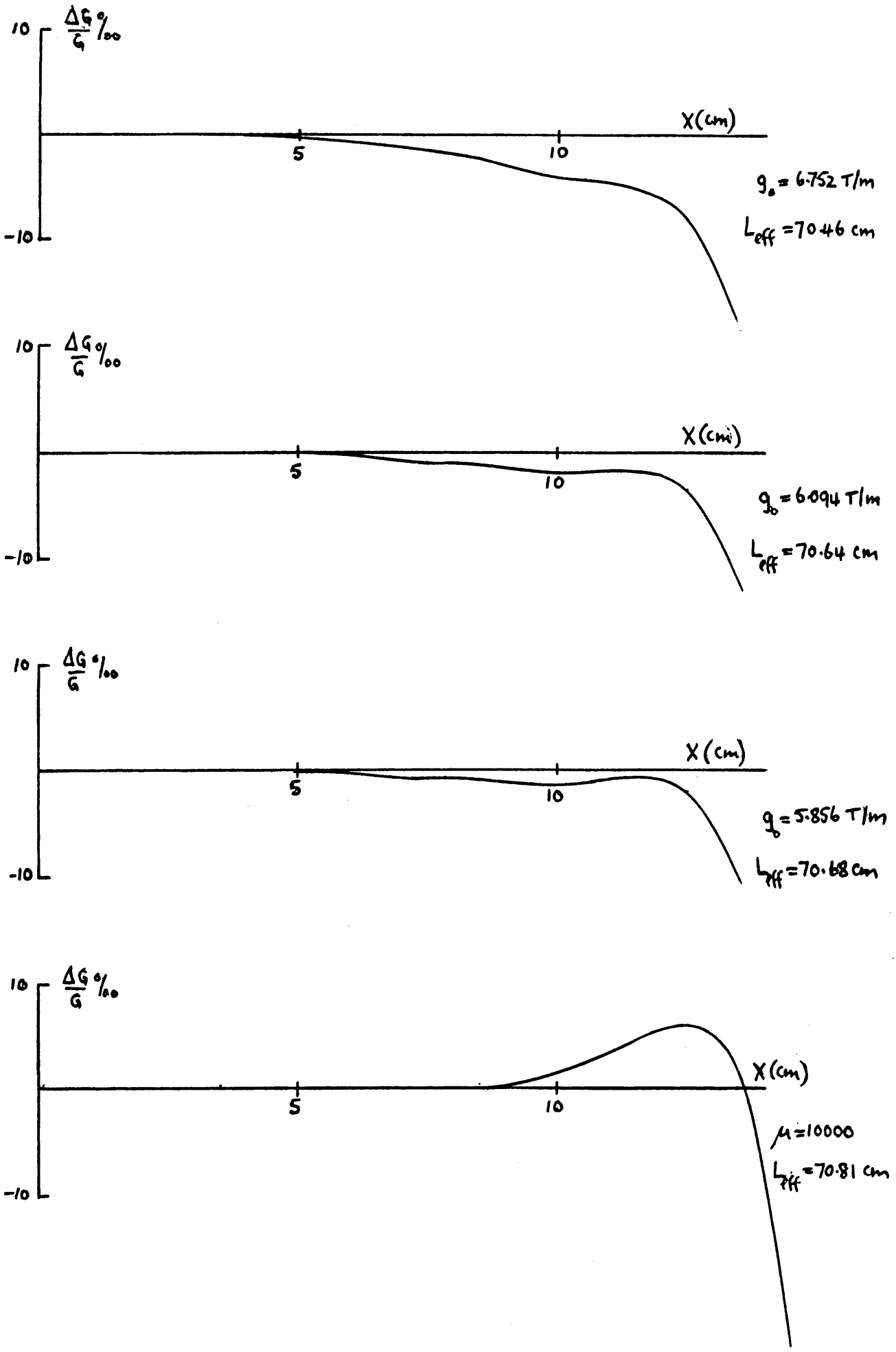

Fig 3. QN results at different energizations

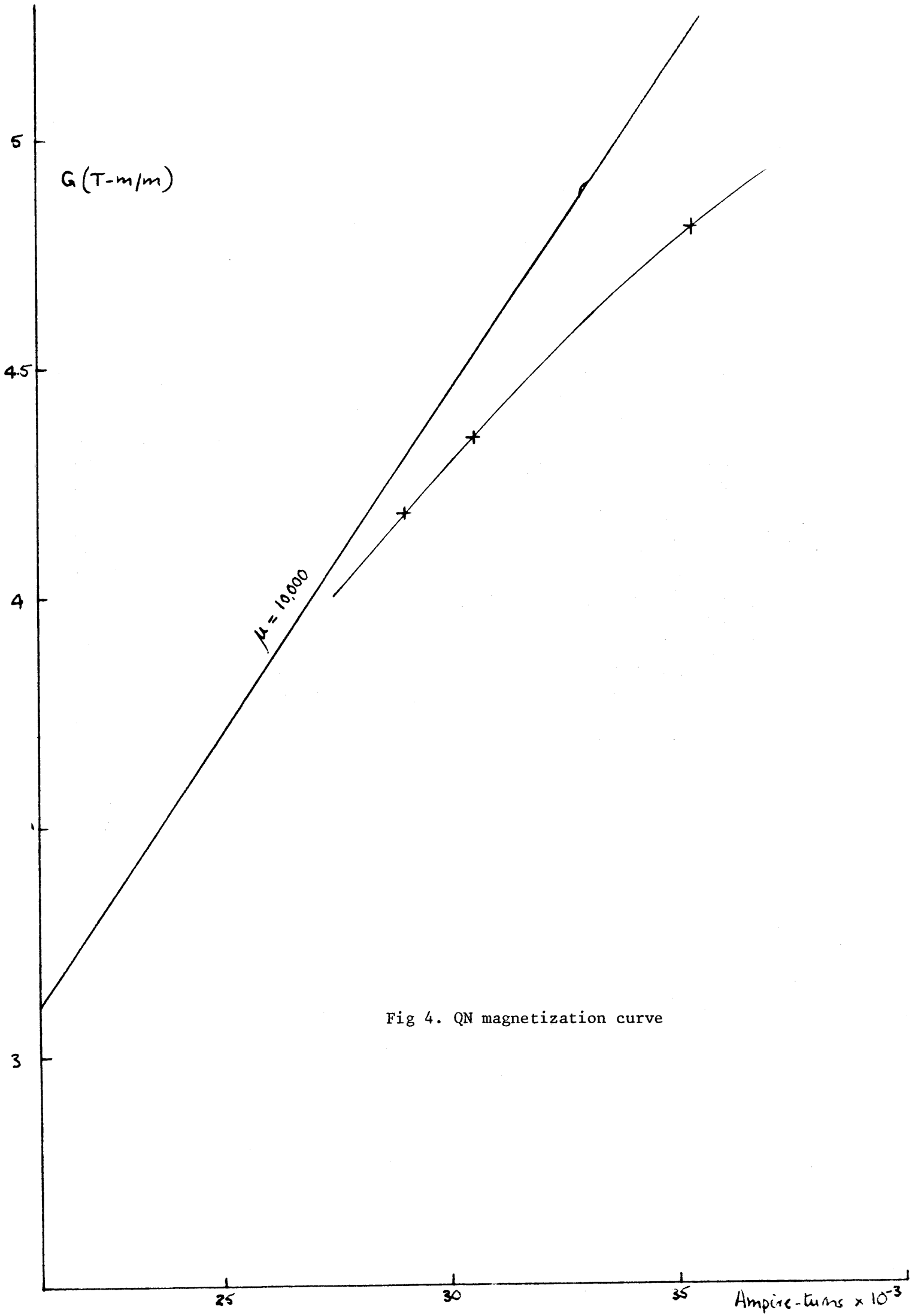

Fig 4. QN magnetization curve

Fig 5.

PROFILE OF NARROW QUADRUPOLE FOR ACOL

POINT	X	Y
D	164.92	35.67
E	173.09	32.31
F	199.31	32.31
G	290	132

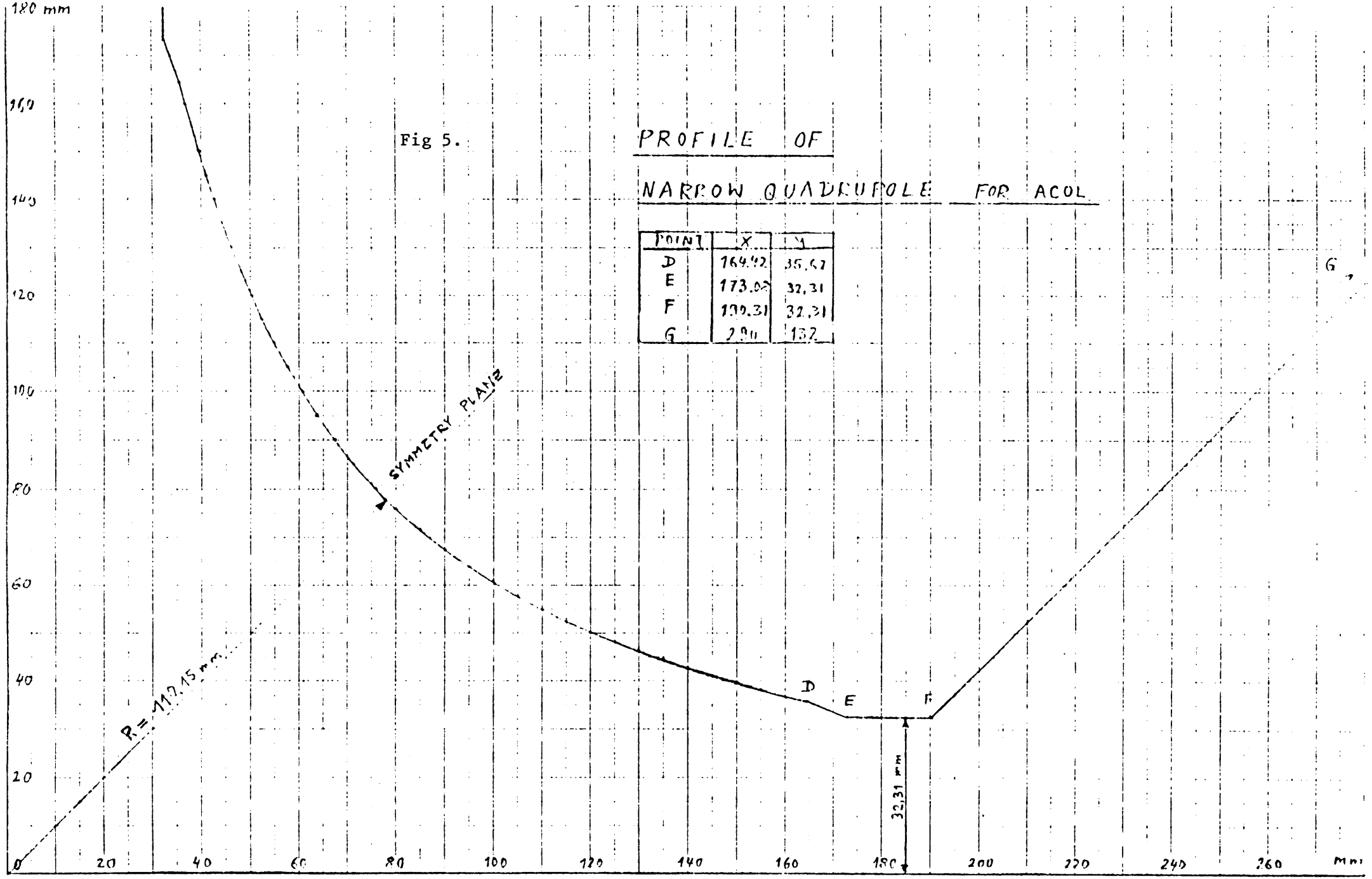

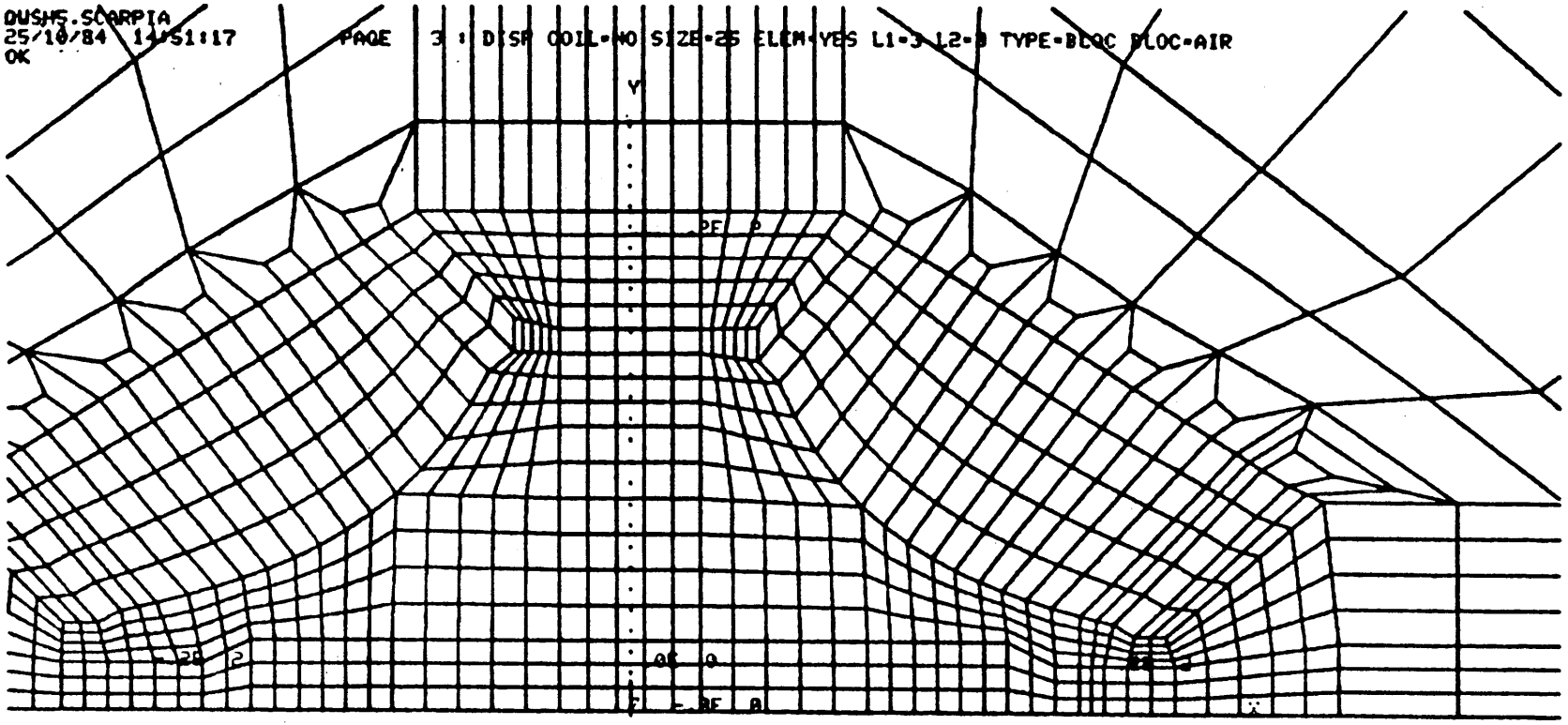

Fig 6. QWS mesh

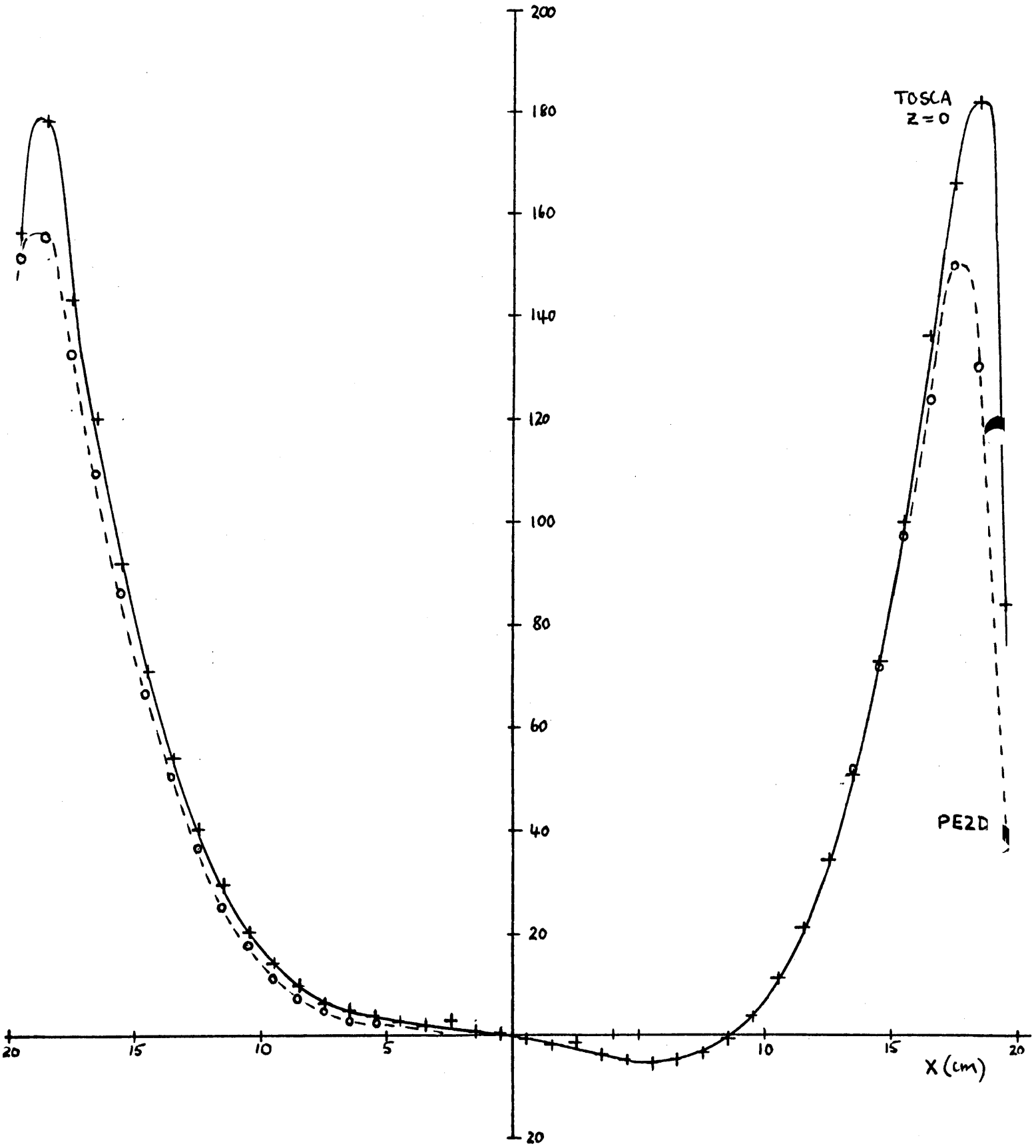

Fig 7. Comparison of QWS on PE2D and TOSCA (z = 0)

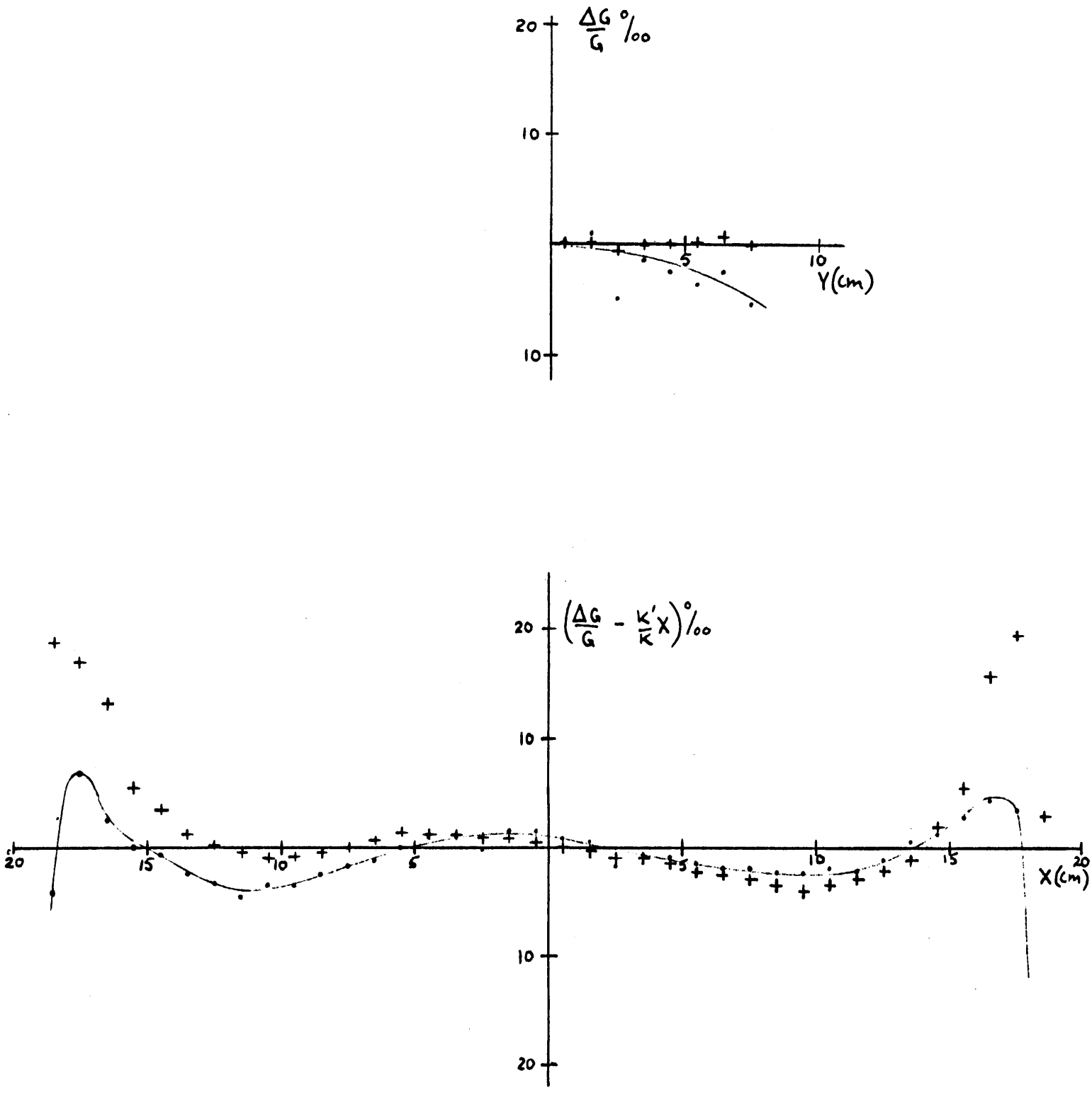

Fig 8. Results for QWS

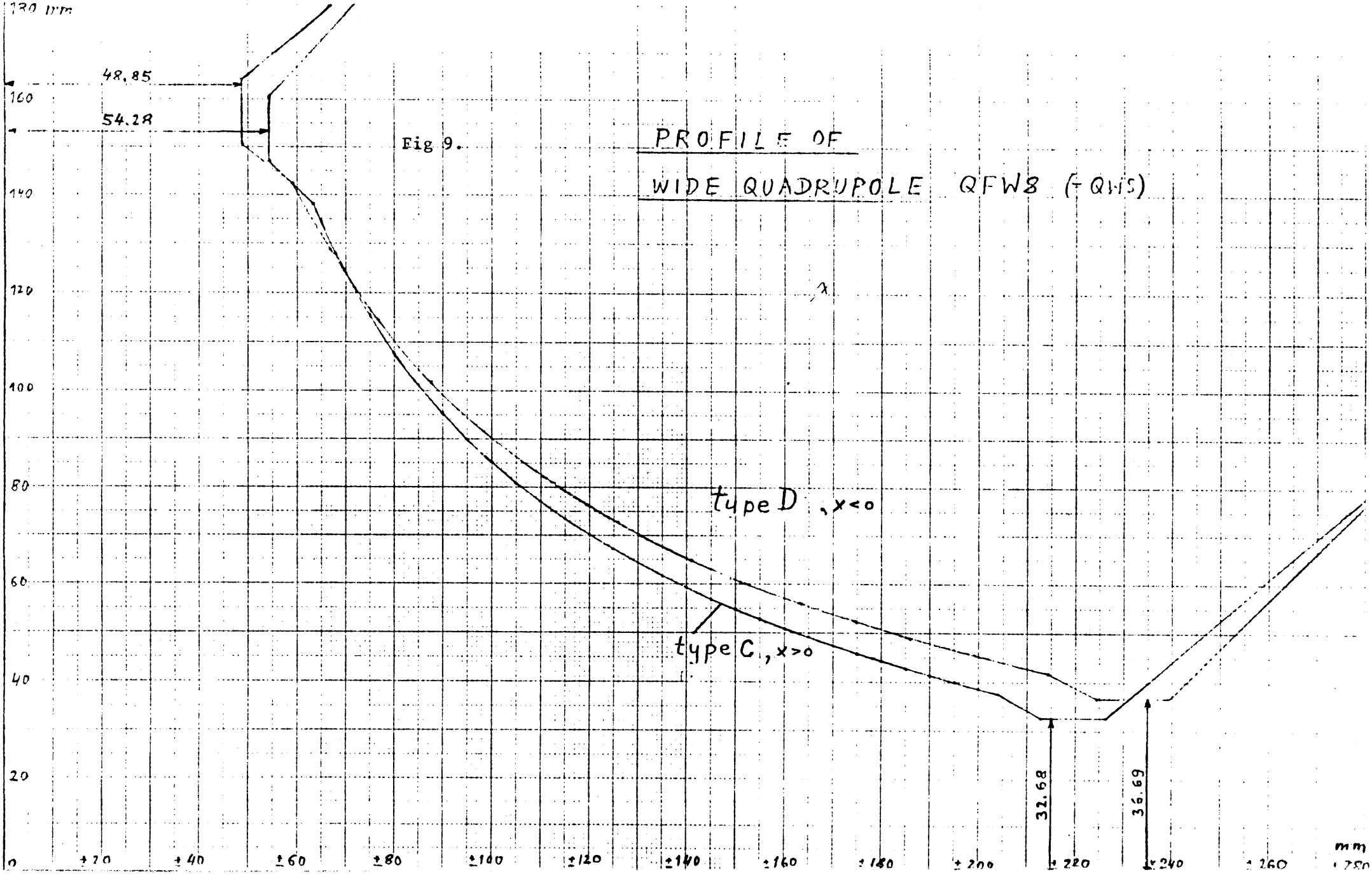
48.85
54.28
PROFILE OF
WIDE QUADRUPOLE QFW8 (=QW8)
type D , x<0
type C , x>0
32.68
36.69
mm

Fig 9.

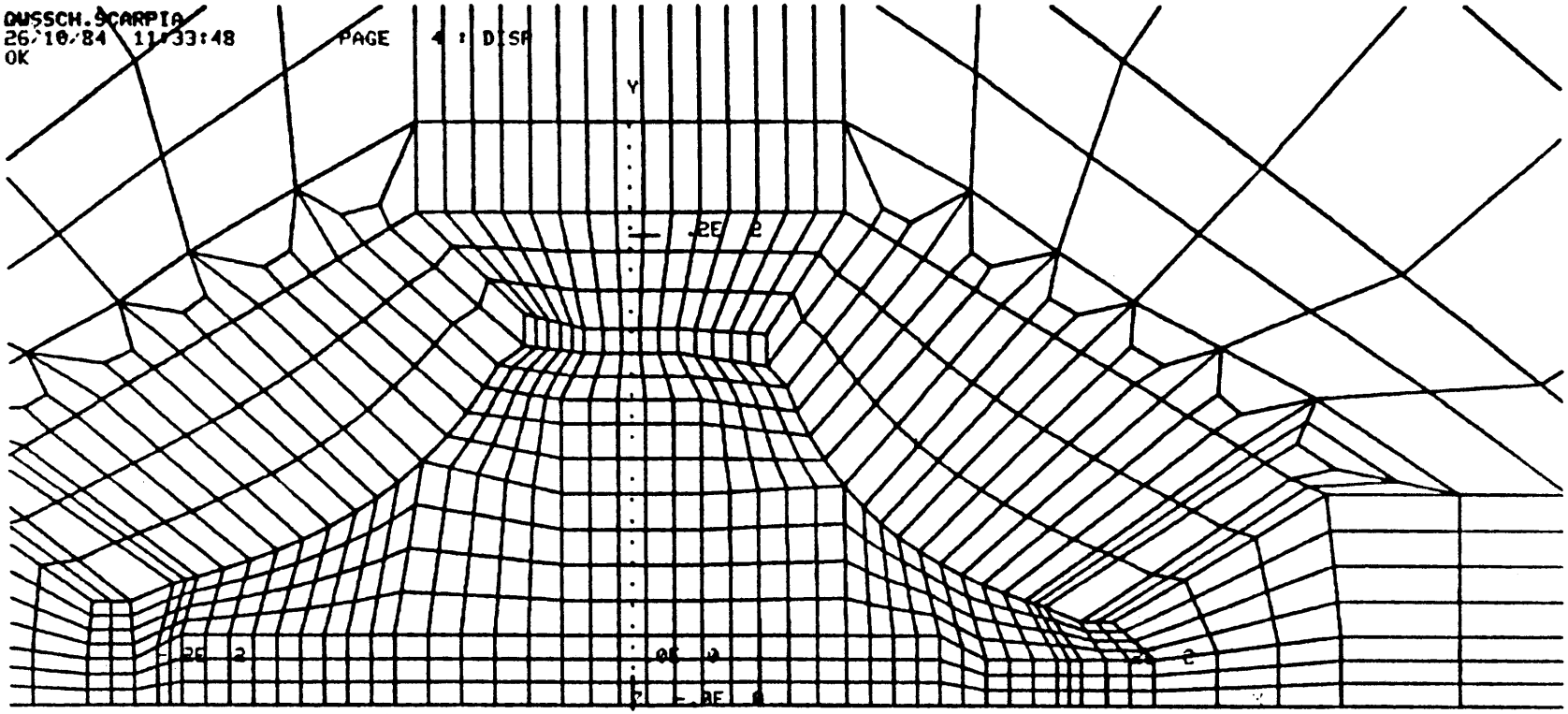

Fig 10. QWS mesh

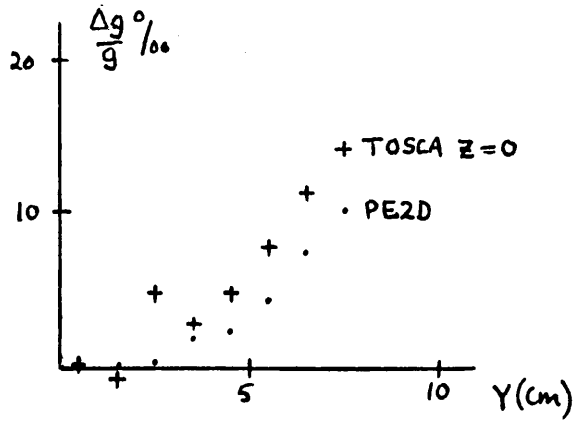

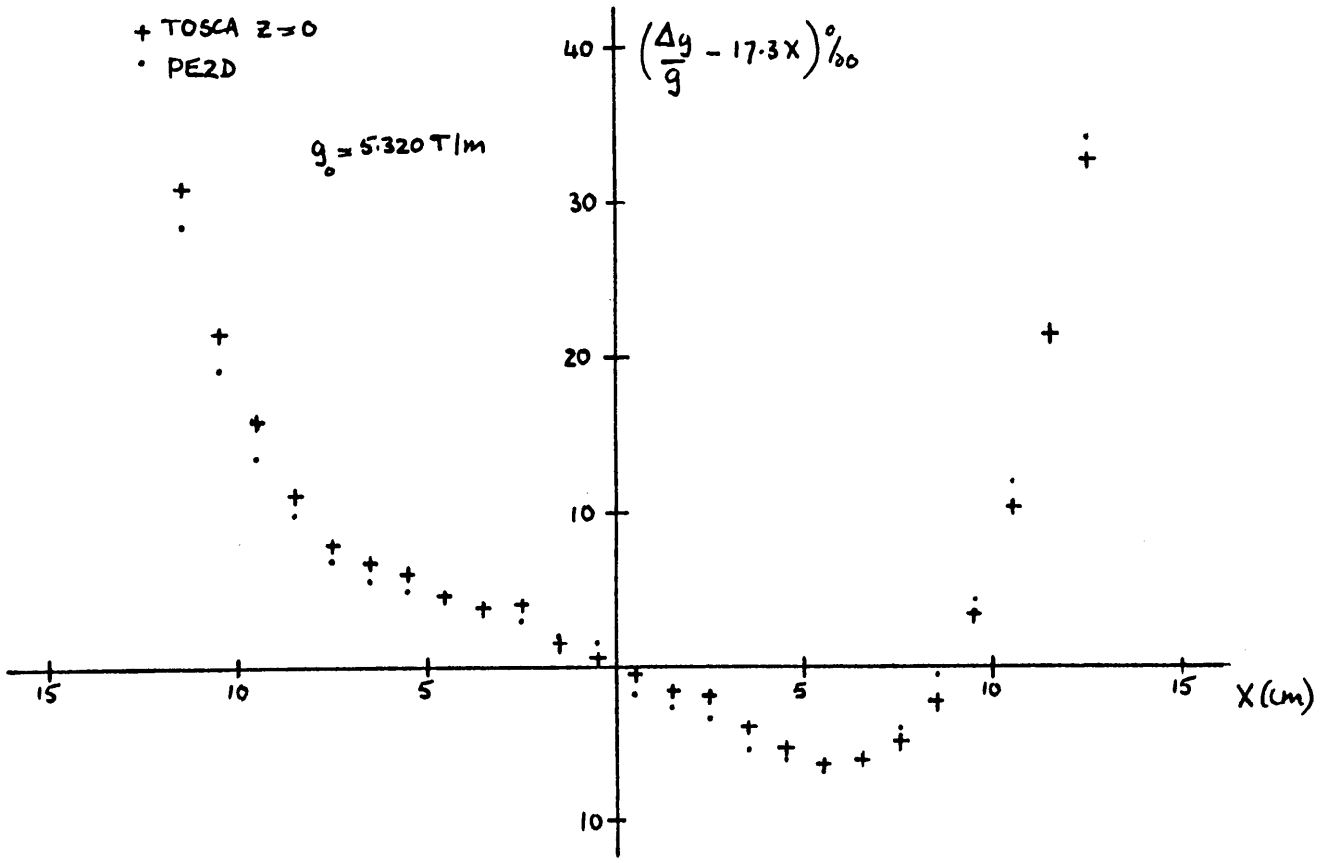

Fig 11. Comparison of QWSS on PE2D and TOSCA (z = 0)

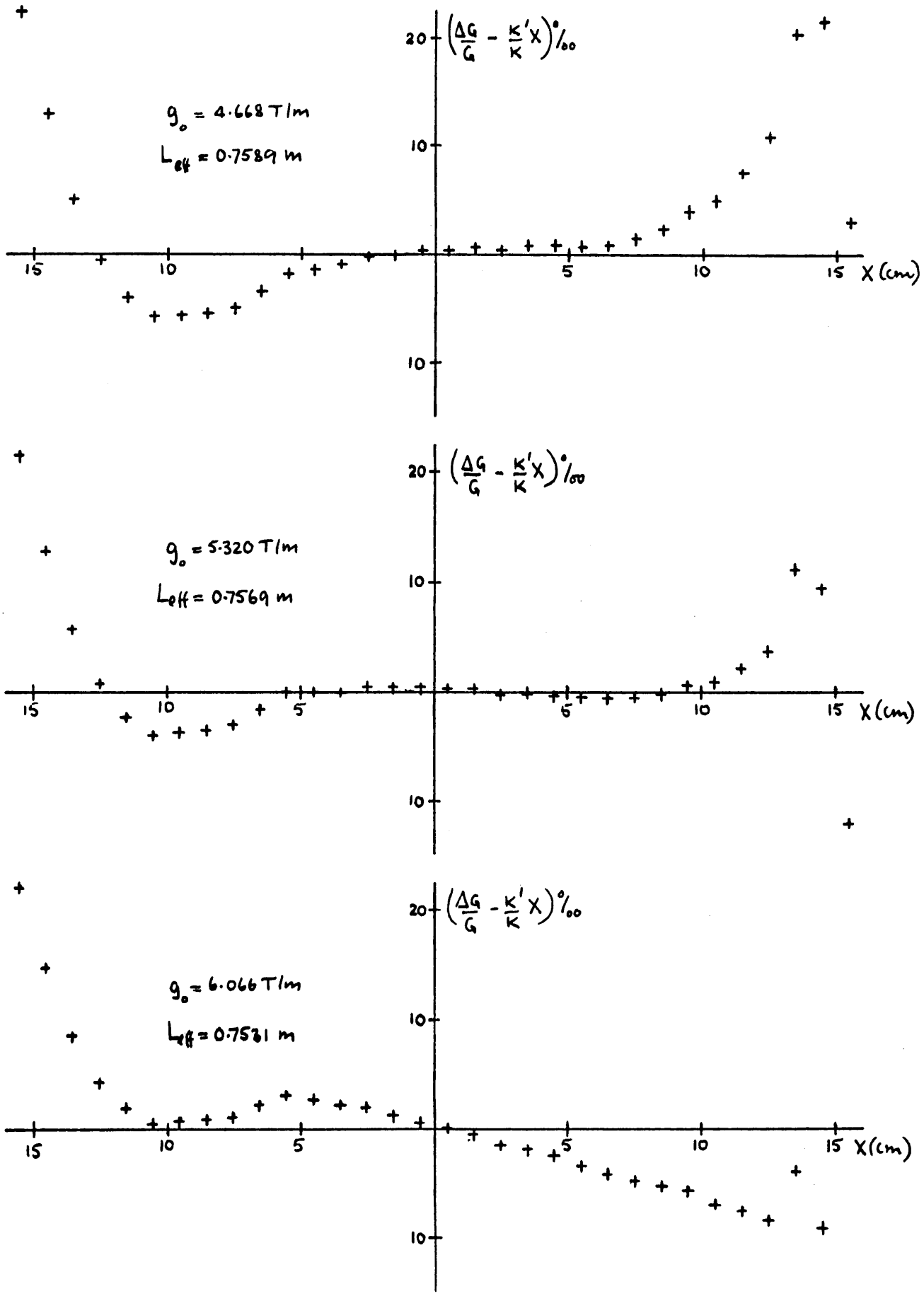

Fig 12. Results for QWSS at three energizations

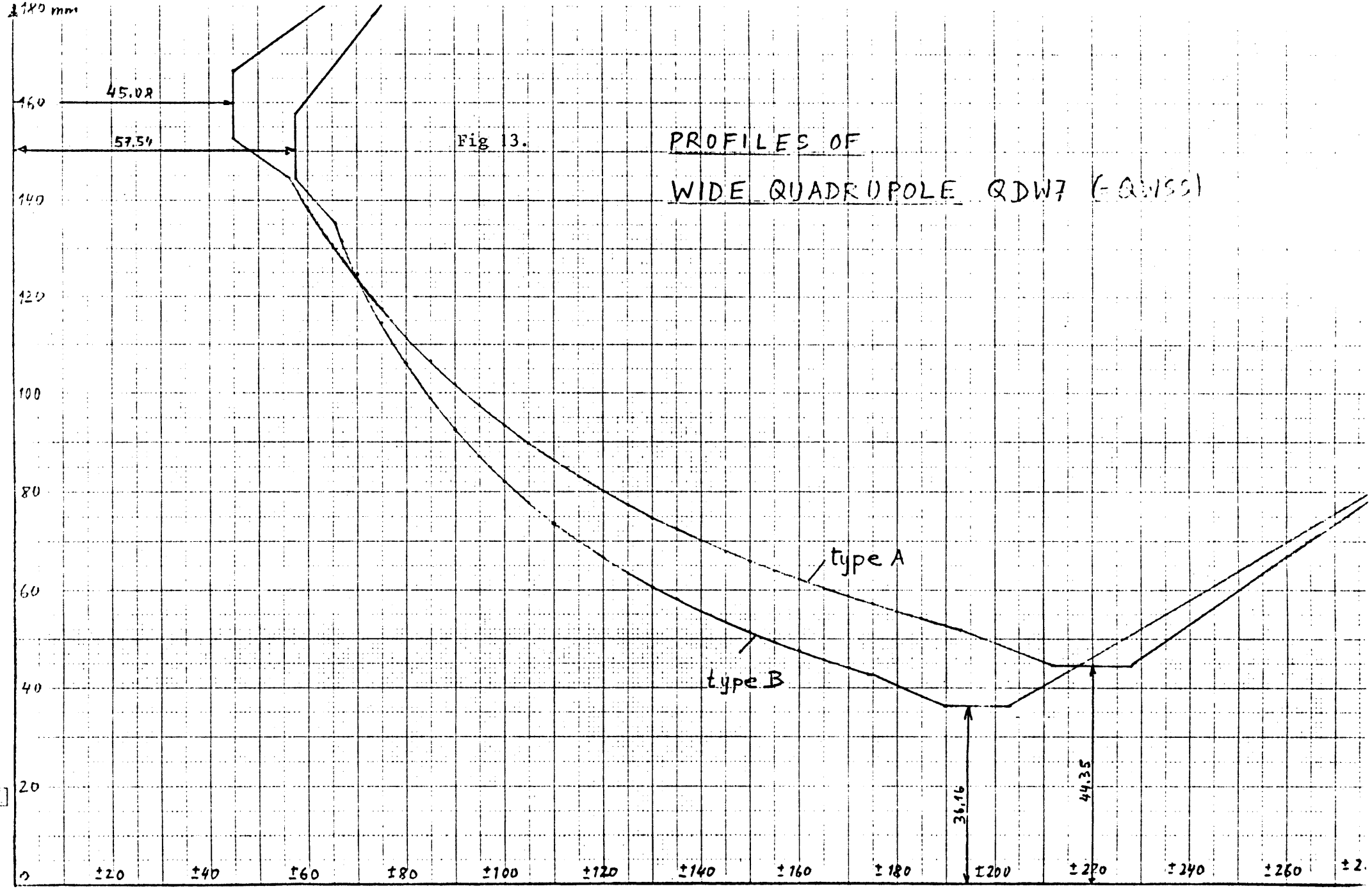

Fig 13. PROFILES OF WIDE QUADRUPOLE QDW7 (-QW1SC)

Before Cutting Sag ± - 25 centre = .25 mm

After Cutting Sag ± - 36 = 0.35 mm

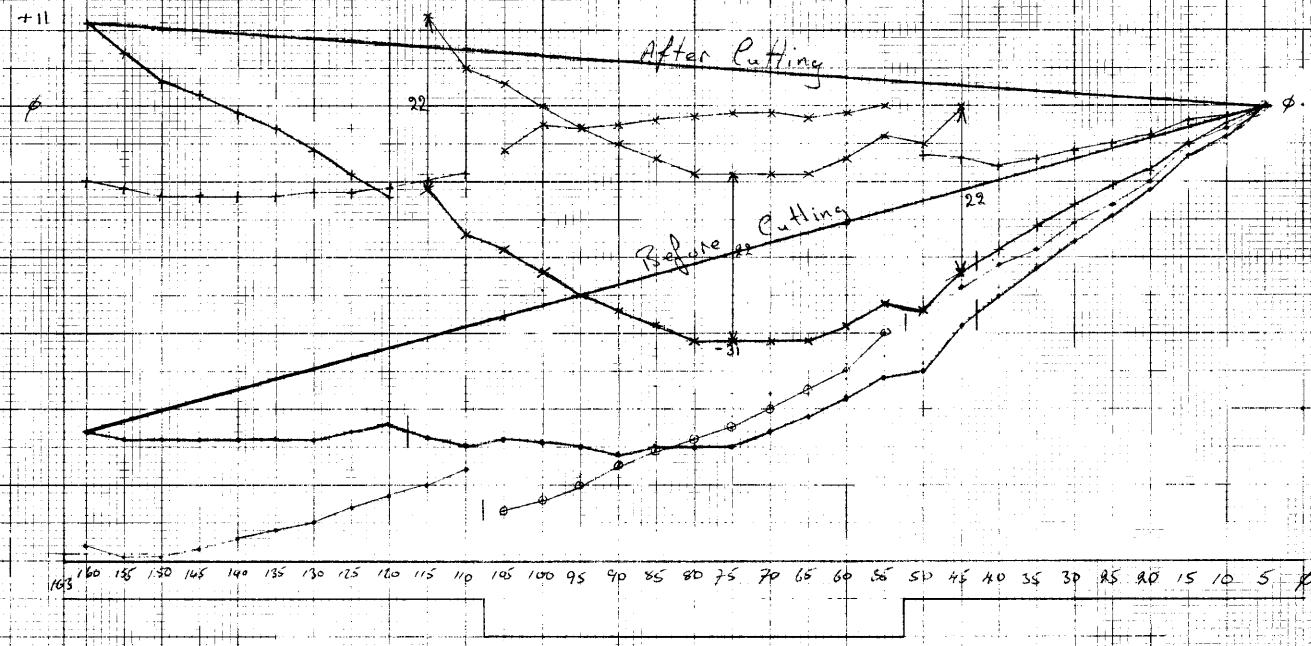

-10 Amps = #49 DISKS 8 CYLINDERS 3,2.

ϕ Amps = "#48,2" "

#49 - #48,2. Diff Done.

Take $\frac{1}{2}(49-48)$